

Petrographic, mineralogical and geochemical characterization of The Tidiennit volcanic complex (eastern Rif)

Mariam Rachidi¹, Samira Adil¹, Mohammed Belkasmi¹, Mohammed Sadequi¹

¹Laboratory of Geosciences, Environment and Associated Resources, Faculty of Sciences Dhar El Mahraz, Sidi Mohamed Ben Abdellah University, Morocco; mohammed.belkasmi@usmba.ac.ma

Abstract. The Tidiennit massif corresponds to a volcanic apparatus that represents one of the two known neovolcanic manifestations in the Nador region (north-east Morocco). It is a satellite volcano of the neogenous volcanic edifices of Gourougou (high-K calc-alkaline to shoshonitic), which is characterized by the presence of various deposits of useful mineral substances (bentonite, perlite). The studies carried out on the Tidiennit massif focused on the bentonites of the three sectors of Prévencia, Trébia, and Taghzoute. The results obtained by EDAX/MEB show that the main components of bentonite are generally: montmorillonite, illite, calcite, hematite, sepiolite, fayalite, albite, biotite, orthose, cristobalite, and calcite, with montmorillonite accounting for a sizable portion of 80%. The studied region was affected by intense striking tectonics. The petrographic analysis of the rhyolitic magma highlights the superposition of two fluidity phases, one linear and the other nested, which is suggested the passage from a plastic to a brittle deformation stage. This favored the evolution of a set of structures and microstructures that facilitated the circulation of water, which allow us to conclude the origin of meteoric and hydrothermal alteration, and that bentonitization (alteration) is closely linked to the lithological characters of the rocks. Keywords: Bentonite, Tidiennit massif, Magmatic fluidity, Spherulite, petrographic, Providencia, Trébia, Taghzout.

1 Introduction

The formation of ore bodies is sometimes intimately interwoven with that of the surrounding rocks and is often accompanied by pneumatolytic or hydrothermal alteration of these rocks, with partitioning of the elements. Conversely, the ore body appears as an intruder in the middle of its geological environment. The purpose of this study focuses on the volcanic and subvolcanic deposits of the Eastern Rif in the Neogene basin of Melilla-Nador, which has several mineralizations of contrasting structural levels (iron skarns, polymetallic Pb-Zn-Ag veins, bentonites, recent hydrothermalism in the form of agglomerates, etc.) [1]. They are associated with the subduction zone and resulted from the crustal shear play of the sinister Trans-Alboran accident [2]. The relationships between mineralization and volcanism are often difficult to define. The primary processes that produce mineralized bodies are plutonism, volcanism, and sedimentation. The processes of weathering and erosion, metamorphism, tectonics, and water circulation are responsible for the transport and accumulation of pre-existing mineralization, whether disseminated or not. Mineralization, which can result from the chemical modification of minerals under the influence of water (from lakes and seas), giving rise to the formation of new deposits, can be modified by external or internal factors. In order to understand the various factors responsible for this phenomenon and this geological diversification in a narrowly confined environment under nearly the same conditions of source and set up,

the scientific goal of this work is to conduct a thorough study of the Jbel Tidiennit stratovolcano massif and the bentonite deposit that characterises it, based on geological, structural, petrographic, and mineralogical studies, as well as geochemical analyses using infrared diffraction and microscopy.

2 Geological setting

The Jebel Tidiennit massif is a volcanic formation from the Miocene, and represents one of the two neovolcanic manifestations of the eastern Rif, which is part of the Eastern Rifian chain [3], extends along the Mediterranean coast from the Nekor fault in the west to the mouth of the Moulouya River in the east [4]. It is a satellite volcano of calc-alkaline to potassium [5] et [6], of the Neogene volcanic edifices of the Gourougou, which are oriented in three directions: NE-SW, N-S, and NW-SE [7], belonging to the calc-alkaline shoshonitic series [8]. It is bounded to the north by the Gourougou volcanic massif, to the south-southeast by the Beni-Bou-Iffrou massif and the Bou-Areg plain, and to the southeast by the Kibdana massif and to the southwest by the Kert basin. (Fig.1) This Vesuvian type volcano consists roughly of banded rhyolite flows on its flanks and is sometimes limited at its base by large, more or less prismatic grayish perlitic outpourings [9]. These flows occasionally have the appearance of perlitic tuffs and are unconformably covered in clear, brecciated layers. Large perlites that later turn into fine-grained rhyolites are occasionally observed. (Fig.2).

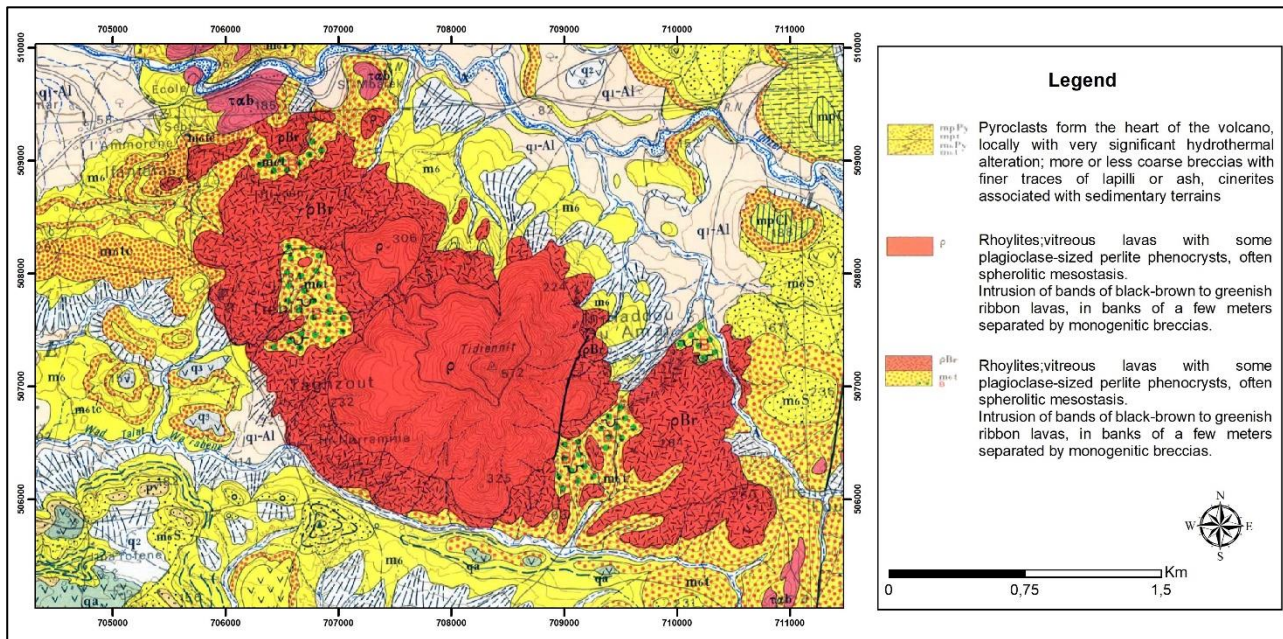


Fig.1. Geological map of the Tidiennit massif based on the ZEGHANGHANE geological carte [10]

3 Materials and methods

The field data were collected from fresh rocks and altered zones. Many samples from different zones were collected from the deposit. Petrography and ore microscopy were completed on polished thin sections from the different facies composing the deposit.

A number of samples of friable and fresh bentonite rock were extracted from the three different deposition zones, with a diameter ranging from 1 cm to 12 cm, which are mechanically processed to generally have a diameter of less than 0.3 mm and introduced into a sample holder for analysis (d: intrareticular distance, in angstroms (Å), θ : diffraction angle).

The samples of bentonite were analyzed for rock data, by City of Innovation and Technological laboratory. Major elements were analyzed by X-ray fluorescence spectrometry (XRF) analysis was performed on bentonite samples using a Philips X'Pert PRO X-ray diffractometer apparatus on Panalatyca powder equipped with an X'Celerator Ultrarapid scintillation detector (Table.1).

The bentonites are characterized by a significant quantity of Smectite [11-12], particularly composed primarily of montmorillonite combined or embedded with kaolinite, illite, and/or other impurities [13-14] The raw bentonite spectrum of the Prévencia quarry was used as reference to identify the different synthesized crystalline phases. The diffraction lines observed was compared to all natural smectites listed in data bases.

Table 1. XRD pattern of montmorillonite clay [15]

Miller index	(001)	(003)	(100)	(004)	(005)	(110)	(210)	(060)	(310)
D(Å)	15.00	5.0	4.50	3.77	3.02	2.58	1.70	1.5	1.24
D(Å)-B1	15.36	5.08	4.49	3.77	3.02	2.57	1.70	1.5	1.24

Infrared spectroscopy, applied to clay materials, makes it possible to differentiate between the water of hydration molecules and the hydroxyls of constitution and to follow the structural changes during acid activation.

Raman scattering spectroscopy is widely used in geochemistry to characterize minerals by their spectral fingerprints, notably by Al-O, Si-O and Mg-O bonds. It allows the identification of minerals, their different phases and their degree of hydration.

EDAX/MEB analysis of the samples aims to determine the composition of crystallites and aggregates present in the samples. Scanning Electron Microscopy (SEM) and EDAX analysis uses an electron beam instead of light radiation as with optical microscopes.

Scanning electron microscopy (SEM) observation gives an image of the morphology of the bentonite with the grain arrangement, bedding, and porosity at different scales of a few tens of nanometers, while the analysis (EDAX) is a method that allows us to know the chemical composition of the material. This technique was carried out on several well-crystallized facies of different dimensions: bentonite, hard rhyolite bentonite and bentonitized tuff.

4 Results and discussion

4.1.Lithostratigraphy

The volcanics surrounding the Gourougou stratovolcano, is composed of numerous volcanics exposed among the sediments of the Melilla-Kert basin, these formations include rhyolitic, dacitic, and andesitic domes and dome complexes with rare basaltic andesites of the high-K calc-alkaline suite.[16]

The Tidiennit complex is a satellite volcano of the Neogene volcanic edifices of Gourougou stratovolcano. A wide range of acid-volcanic formations are clearly observed, in the complex, comprising a set formed by tuffs, polygenic breccia, and several rhyolitic flows, which are more or less banded, fine-grained cryptocrystalline, and often granular upwards [16,18,], framed by Messinian volcano-sedimentary formations, discordant pyroclastic levels interspersed with marl. [15] Thin sections of the rocks were studied microscopically, and DAX/MEB analysis was conducted to determine their nature and genetic relationship to the associated bentonite deposits.

Petrology of the parent rocks: A summary of the petrographic and geochemical characteristics of the main units of the set of rocks forming the massif, where we recorded the continuity of five major intrusive and extrusive lithofacies, mainly distributed in circular (Fig.2), from the center to the border we find:

- **Rhyolite:** this is the most present facies of the massif, occupying almost the entire massif, located in the center of the intrusion (Fig.2), with a light grey to reddish color. It is characterized by the presence of an arrangement in the form of banks (or false stratification), which reflects the viscosity of the magmatic flows. As can also be seen in the perlitic rhyolite, the bedrock of bentonitization, it outcrops adjacent to the rhyolite generally in massive form, showing in places a clear fluidity and a very reliable nature testifying to the very high degree of alteration with a color very close to the surrounding bentonite, inferring a very advanced degree of bentonitization (Fig.3A).

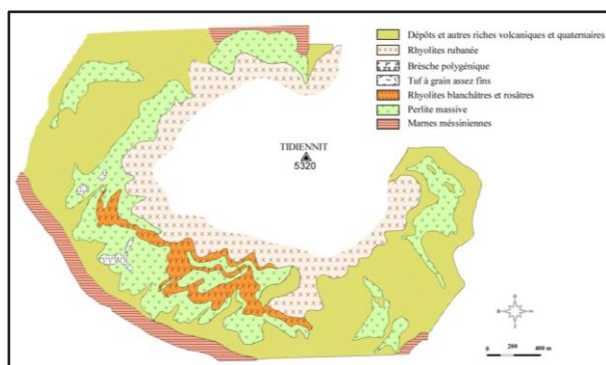


Fig. 2. Schematic map of the southern flanks of Tidiennit complex [20]

- **Perlite:** The main deposits are located on the southern and southwestern flanks of Jbel Tidiennit. Macroscopically, five groups of perlite rock facies can be distinguished: massive, obsidian, granular, brecciated and banded [19]; exhibiting various degrees of weathering. It occurs as grey, greenish or blackish hydrated glass [21]; microscopic observations of this facies are characterized by the presence of frequent cracks and fine fractures, showing zones of weakness or the beginning of bentonitization.

- **Volcanic tuff:** of the Tidiennit complex outcrop in the form of panels to the south and south-west, with a

diffuse, low-percentage contour vein, chaotic and monogenic aspect (of volcanic origin), they show a normal grain-graded sequence; horizontal stratification in places, heterometric with the presence of metric lenses with more or less fine elements; they are characterized by a color ranging from white to light brown or green. In the field these tuffs can be shown in places to be consolidated into pyroclasts which are quite hard with siliceous cement (chalcedony filling) and are generally friable (Fig.3.B). It is formed by the accumulation of volcanic projections of millimeter-sized fragments, minerals and rocks, as well as whole minerals, which gives it a brecciated appearance, the binding of which is the result of a highly developed alteration of a clayey nature.

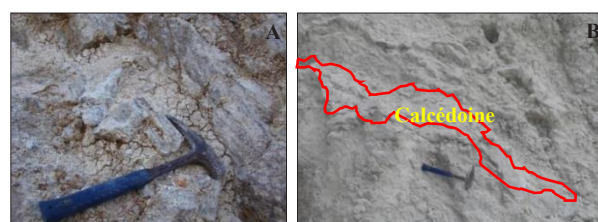


Fig.3.A): Field photograph showing tuffs with pseudo-fluid structure with a bed of chalcedony
B): Field photograph showing a bentonized banded perlitic rhyolite

- **Breccia:** Tectonic monogenic breccia of variable size at the level of faults. The volcanic origin of the area is the factor responsible for the production of another type of volcanic breccia resulting either from re-moving explosions of lava whose crust had already congealed or superficial collapse.

- **Bentonite:** this is the product of alteration that has affected the facies; rhyolite, especially perlitic rhyolite, and perlite. The fact that this region has undergone intense tectonics influences these facies by showing, in most cases, breaks that present areas of weakness that make them fragile and facilitate the circulation of water, which constitutes the main agent and responsible for this phenomenon

4.2. Geochemistry

The complete geochemical (major) analyses of the Rhyolites are compiled in (Table 2). The position of the rhyolites in the K_2O-SiO_2 diagram (Fig.4) shows that they have SiO_2 -rich compositions, compared to basaltic andesite and dacite. Perlitic rhyolites are the bedrock of bentonitization; they generally crop out in massive form, presenting a very clear fluidity in places. Their very reliable nature testifies to the degree of very high alteration, and their color is very close to that of the bentonite that surrounds them, which deduces a very advanced degree of bentonitization.

They thus show some depletion in percentage K_2O ; essentially linked to the alteration of the Rhyolite. The major element spectra (Fig.5) of Rhyolite samples show high LILE/HFSE ratios and low Nb contents (negative anomaly) which are characteristic of calc-alkaline lavas [22], these spectral patterns are common in orogenic zones [23-24]. The negative Nb anomaly is more

pronounced for the rock, as fluids produced by dehydration of the subducted crust carry trace elements that enrich the magmas formed. the negative anomaly of Nb possibly reflect some crustal contamination. [25]

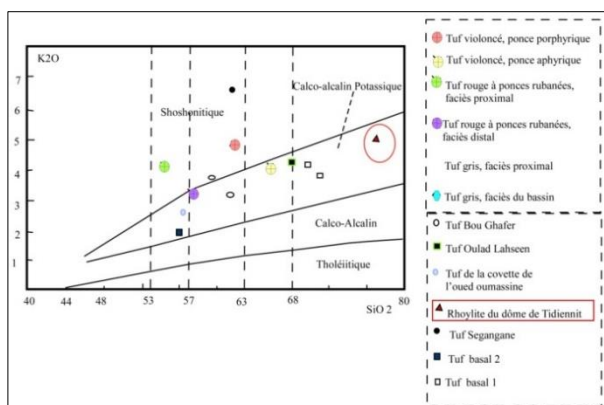


Fig. 4. Position of rhyolites in the K₂O-SiO₂ diagram [5]

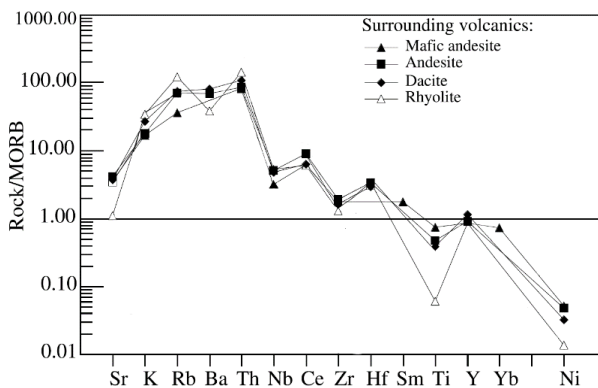


Fig. 5. MORB-normalized spidergrams [26] for representative samples of the Gourougou. [16]

All the lavas develop a negative Ti anomaly, indicative of Fe-Ti oxide fractionation. The amplitude of this anomaly is more marked in the rhyolite. The richness of the rhyolites in plagioclase with a low K₂O content, allows us to suggest that the genesis of the rhyolites is related to an evolution fractional crystallization of a basic calc-alkaline magma rather than an origin by anatexis. (Table2)

Table 2. Chemical analyzes of Rhyolite Jbel Tidiennit, Eastern Rif [5]

Elements	SiO ₂	TiO ₂	Al ₂ O ₃	Fe ₂ O ₃	MgO	CaO	Na ₂ O	K ₂ O	H ₂ O	Total
EchT	77.06	0.09	12.59	1.10	0.0	1.01	3.37	5.02	0.73	100.99

4.3. Petrographic characters

Microscope observations showed the parent rocks to be rhyolite, perlite, and Tuff pyroclastic which in the rhyolite, magmatic fluidity is the most favorable structure that leads to the production of bentonitization, which is well marked in the fluid porphyry hyaline texture, where it is more developed than in the hard compact spherulites structure that makes alteration more difficult, and it can be said that bentonitization follows the fluidity of the rock. The perlitic facies has fine cracks which are among the structures that favor bentonitization and are well developed in tectonic

zones; zones of crushing of faults that make it more reliable and facilitate attack by alteration agents (Fig.6A). The reliable appearance of pyroclastic tuffs favors bentonitization which turns from a greenish to whitish color in the massive case to a reddish color. The well-developed bentonitization at the mesostasis level, the phenocrysts are also affected marked by alteration that follows the contours, generally starting from the center towards the edges and following the cleavage planes and/or zoning in the case of orthoclase (Fig.6. B&D).

Fluidity is a preferential vector orientation organized by the deformation of the viscous matrix: it is therefore a revealing structural marker of magmatic to finite-magmatic deformation [22] [27]. The facies of the Tidiennit massif are essentially formed of quartz, potassium feldspar (CF) and biotite. The study of the fluidity is carried out especially on the potassium feldspar (CF) allows us to draw several criteria such as:

- Polysynthetic twins are parallel to subparallel along the crystals and can show zoning, are marked for plagioclase by folded, flexuous forms also note microfractures which are frequent, so we can deduce that the facies have undergone to the two phases; that follow; marked by the passage of a stage of plastic deformation to a brittle deformation stage. In addition, the plagioclase has undergone a strong alteration that allows the development of sericite. (Fig.6. C)

Microscopically the shear bands form a discontinuous network, very fine with a size limited to 0.5 mm, especially at the level of the feldspar (plagioclase) phenocrysts, rarely observed at the level of the other crystals, potassium feldspar, biotite and quartz. (Fig.6.C)

- The fragments are offset by a few micrometers, showing reddish porous altered networks at the LPNA with a salty appearance as well as intra-crystal fracturing on both sides of this band which facilitates the clear alteration. Generally, it is the dexterous ones that develop better.

- Feldspar phenocrysts intersected by shear bands are rare to encounter, explained by the existence of a strong ductility contrast between the crystals and the microlitic mesostasis in rhyolites with microlitic texture as well as in perlite. (Fig.6 F&E)

- The quartz is the last mineral to crystallize, it is the most suitable, the most ductile; it is therefore the first to record a deformation in the solid state at high or medium temperature, microscopically and appears in the form of:

- ✓ The spherulites, which give the rock a spherulitic appearance, are among the main parameters of the fluid rhyolite found in this area. Mostly composed of quartz spherulites, it is a partially recrystallized glass in the form of spherical aggregates of fibroradiated minerals (spherulites), represented mainly by quartz spherulites. Crystallization of rhyolite liquids gives rise to spherulitic fluid rhyolites, spherulitic rhyolites, as well as fully glassy rocks. (Fig.6. G & H)

- ✓ The sub-automorphic to auto-morphic phenocrysts suggests that it has not undergone solid

state changes. Fluidity can be interpreted at the grain scale in volcanic rocks, frequently traced by microlites that are well noticed in biotite crystals as elongated rods accommodated by microlitic-looking quartzofeldspathic mesostasis (Fig.6J)

▪ Glass shards are very rare, found in rhyolite thin sections. They are characterized by a variety of petrographic features; generally, have a glassy-clastic character due to the accumulation of glass shards that are mostly X-, Y-, or L-shaped, [28] which may be the result of the bursting of the walls of vesicle magma. Their devitrification during cooling indicates their pyroclastic origin, manifested by crystal formation and

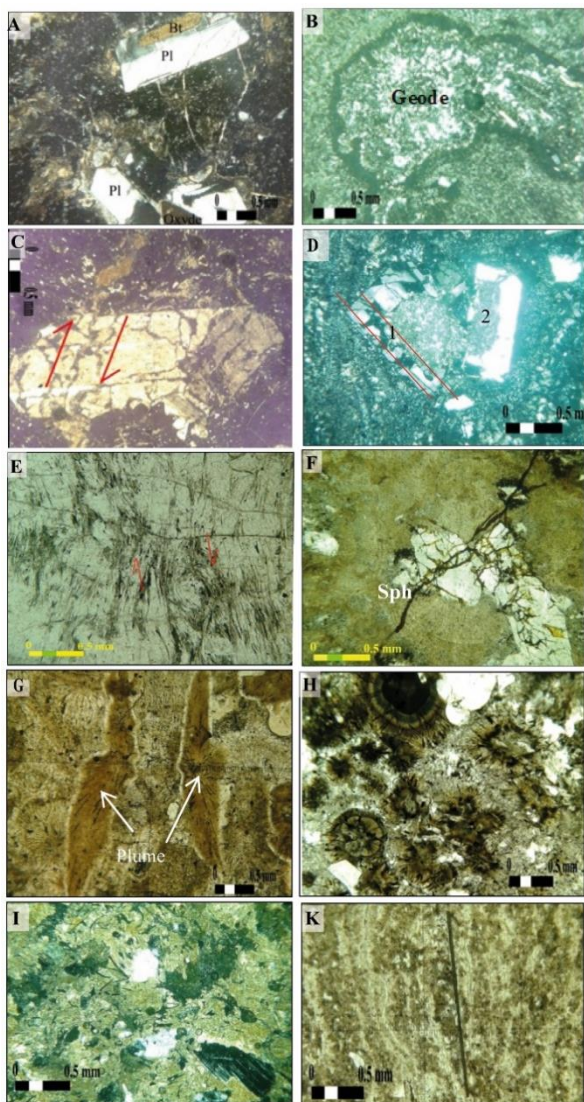


Fig.6. Photomicrographs of typical parent rocks; the rhyolite with a spherulitic texture. A) Occurs in the pearlite at the level of fine cracks. B) At the edge of the quartz recrystallization geode. C) LPA: highly charged feldspar with a bentonitized dexter shear band. D) Well developed at the mesostasis level follows the civate(1) and (2) zoning planes. E) LPNA: fluid pearlite with a shear band F) LPNA: fluid pearlite with a shear band. Rhyolite with a spherulitic texture: (G) in the form of feather H) in the in the oval form. (Sph: spherulite) I) Photomicrographs of the rhyolite: the glass shards in X and Y form. J) Elongated biotite rod traces the fluidity of mesostasis microlites.

loss of transparency. Pyroclastic flows are dense gravitational currents of gases and particles frequently generated during volcanic eruptions. (Fig.7 I)

5 Mineralogy of bentonites

a. SEM observations

The results obtained from the EDAX/MEB analysis confirm the microscopic studies that were carried out on the same sample showing the presence of two mesostasis in addition to the argillation that takes place intra- and inter-sheet (Fig.7 & 8).

A well-marked heterogeneity by the presence of the debris of xenomorphic rocks, in which recrystallization begins to develop in the form of a quartz micro-geode.

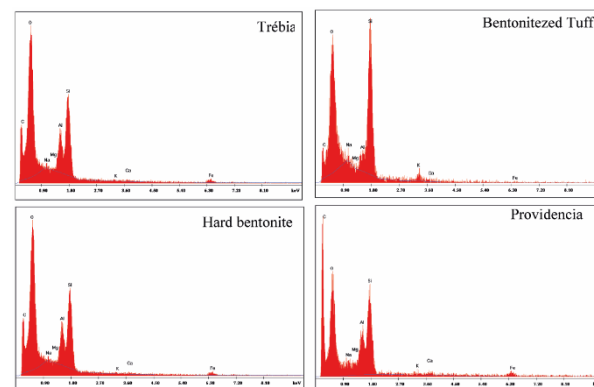


Fig.7. Diagram showing qualitative analyses by EDAX of bentonite

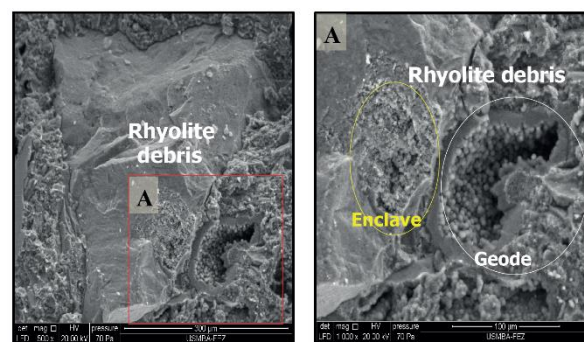


Fig.8. Selected scanning electron microscopy (SEM) images showing the micromorphology of representative bentonite samples: A) MEB tuf bentonitised

The development over time of the hydrated calcium silicate hydrates or calcite (CSH) in the sample are observed, they have a fibrous form which is clearly observed in (Fig.9).

The vibration bands of the characteristic bonds of the bentonite in the massif are shown on the infrared spectrum (Table 3&4) (Fig.10).

The diffractogram of the Providencia bentonite sample shows a polyphase clay mineral. The lines reveal a dominance of peaks characteristic of Montmorillonite well-marked by the presence of a peak with $d(001) = 15.92 \text{ \AA}$ important and very intense (3453.36). The characteristic lines of Illite: (9.95 \AA). It also shows the characteristic lines of sepiolite: (12.57 \AA), the characteristic lines of calcite; (3.02, 2.51 \AA), the

characteristic lines of hematite; (1.69, 1.49, 1.43, 1.29, 1.24, 1.21), orthoclase lines: (3.91, 3.63, 3.14), Albite lines: (6.22, 4.04, 3.77 and 3.20), and quartz lines: (3.34 and 2.23 Å) which are rarely present in the sample. Quartz (α -SiO₂) and feldspar (NaAlSi₃O₈) considered as non-clay phases, are colloidal impurities and cannot build up a clay nature (Table 3&4).

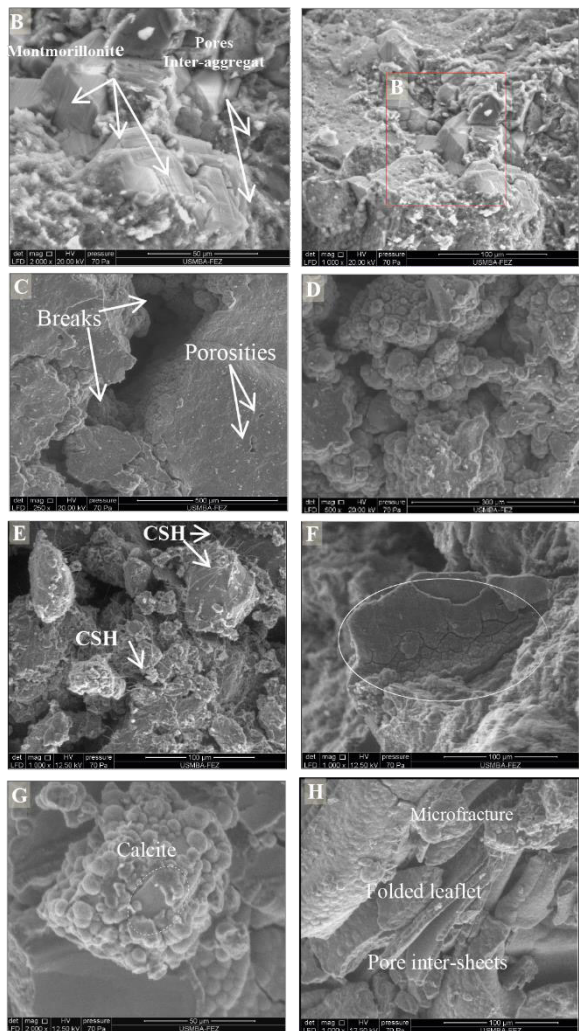


Fig. 9. Selected scanning electron microscopy (SEM) images showing the micromorphology of representative bentonite samples: B) Photo of the MEB showing a cluster of interlocking minerals C) showing the appearance of mesostasis in a dur bentonite with a laminated structure.

Table 3. Mineralogical composition of massif Tidiennit bentonite samples

	Providencia		Taghzout		Trebja	
			E1	E2	E3	E4
Montmorillonite	76		74	76	80	81
Quartz	-		-	-	1	1
Illite	-		-	-	1	1
Sépiolite	-		7	8	1	3
Albite	-		6	5	4	4
Biotite	-		-	1	-	-
Orthose	4		2	3	5	6
Cristobalite	5		1	1	-	-
Calcite	13		3	2	6	3
Fayalite	-		-	2	-	2
Hematite	2		7	2	2	1
Sanidine	-		-	-	-	3

Table 4. XRD diffraction ‘d’ values of clay fraction

d(Å)	Possible mineral
15.38203 - 2.56014 1.49269- 1.79552 -1.24178	Montmorillonite
2.23487- 3.34763	Quartz
9.95269-9.99549	Illite
12.28979 -4.45727	Sépiolite
6.39463-4.1622-3.74403-3.62268-2.28981-1.98853	Albite
3.36253	Biotite
3.21577-3.17847-1.45225-2.03146	Orthose
3.12846-2.34797-3.00405	Cristobalite
2.84171-2.49191-1.56338-1.8288	Calcite
2.94479	Fayalite
1.71658-1.69448-1.59556-1.28888	Hématite
3.74409	Sanidine

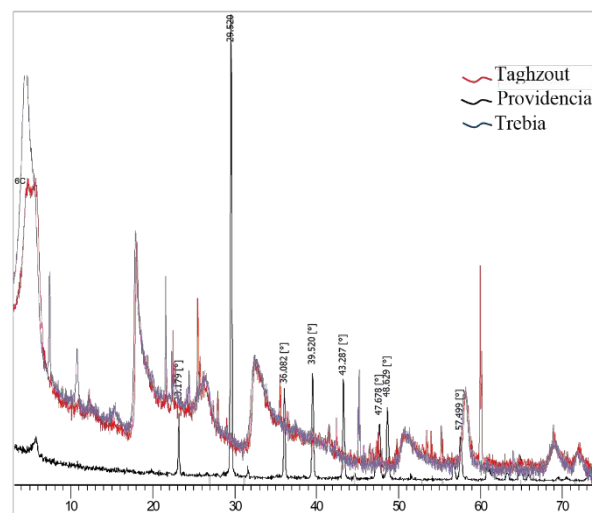


Fig. 10. Representative XRD patterns of bentonite samples from the Tidiennit massif

The fact that the analyses gave the same results, we were satisfied with the analysis of the Trebja bentonite (Fig.11), while keeping the others as appendices. The results are as follows:

Si-O bonds: Si-O bonds are the strongest bonds in the silicate structure and can be easily recognized in the infrared spectra of these minerals by intense bands. They appear in montmorillonite between 1200 and 900 cm⁻¹ which is generally centred at 1108 cm⁻¹ (shoulder) [29]. In our case this band appears at several peaks 986.25, 915.38 and 1108.84 cm⁻¹ in the different samples of the Prévencia sector. The presence of trivalent ions in the tetrahedral sites which substitute for silicon and ferritic ions in the octahedral sites which disrupt the Si-O vibrations are responsible for the shift to lower frequencies. For the deformation of the Si-O-Al bond manifests itself for montmorillonites by a peak at 550 cm⁻¹ which marked in our sample at 591.87. While the 514.62 peaks present the vibration bands of the asymmetric Si-O bond [31-34], these bonds are generally presented at the silicate mineral Quartz.

O-H groups are generally characterised by two absorption regions between 3800-3000 cm⁻¹ characteristic of montmorillonite [13], and between 1700-1600 cm⁻¹ correspond to presence of the water in the mineral [32-36]. Analysis of the Prévencia samples shows that the band at 3625.38 cm⁻¹

corresponds to the valence vibrations of the structural O-H groups bound to Aluminium (Al-O-H) or magnesium [36-39] appearing precisely in the montmorillonite structure, while the band at 3391.05 cm^{-1} corresponds to the vibration of the bonds of adsorbed water [13], and those at 1633.16 cm^{-1} correspond to the O-H deformation vibrations of the bonds of the adsorbed water molecule between the sheets. [36-42]

Table 5. Important IR bands of clay along with their possible the Tidiennit massif

Assignments	OH stretching vibration zone (cm^{-1})
3620.45, 3686.7, 3625.45, 3686.7	Al-Al-OH
3620.45, 3623.02	Al---O-H (inter-octahedral)
3377.95, 3395.04	H-O-H str.
1632.45-1634.53	H-O-H str.
1109.28, 1111.75, 1101.97	Si-O-Si, Si-O str.
915.38	Al---O-H Str.
705.05, 712.79, 787.42	Si-O str., Si-O-Al str. (Al, Mg)-O-H.Si-O- (Mg, Al) str.
512.83, 514.51, 520.09, 516.22	Si-O astr.

Y-OH groups: The elongation band of the H-O bound to Al-Mg [43-44] appears between the regions from 950 cm^{-1} to 600 cm^{-1} corresponds to the deformation vibration of M-O-H. In our case it is observed in the following range; 797.11 cm^{-1} . The nature of the cation to which the hydroxyl group is bound directly influences the position of this band.

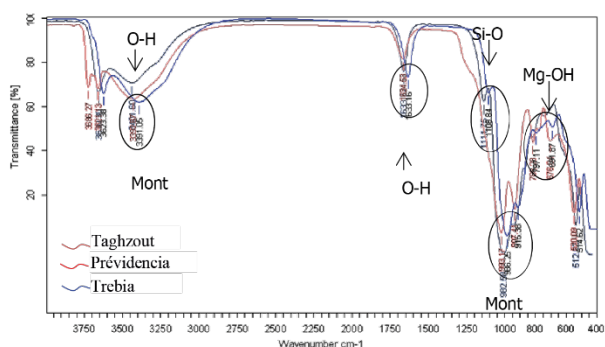


Fig. 11. FTIR spectra of bentonite the Tidiennit massif

All of the above mentioned OH and Al-OH vibrational bands are inactive in the Raman.

b. Raman scattering spectroscopy

The spectra of the analyses are compared with the reference spectrum which confirms the same results obtained from the other analyses that were carried out. Thus, the Trebia bentonite contains a significant amount of montmorillonite, around 80% of the main phase. (Fig.12)

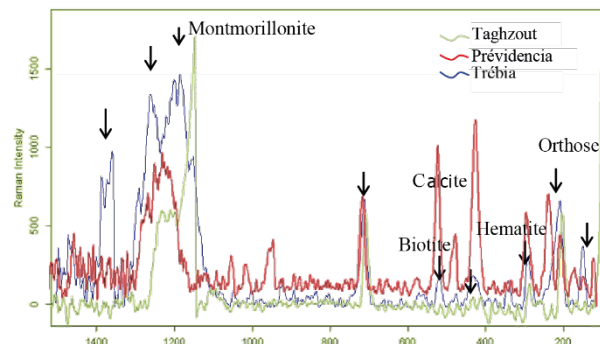


Fig.12. Raman spectra diagramme of bentonite the Tidiennit massif

6 Conclusion

In the Tidiennit massif, the main results concerning bentonite can be summarized as follows:

The geochemical study of the rhyolites shows compositions of the magmatic series of potassic calc-alkaline type.

The petrographic and structural study allowed us to conclude that: (i) the rhyolitic magma shows a clear linear magmatic fluidity superimposed on a second imbricated fluidity. (ii) The strong ductility contrast between the crystals and the microlitic mesostasis can be explained by the succession of two phases marking the passage from a plastic to a brittle deformation stage.

The study area underwent intense brittle tectonics which favored the evolution of a set of structures and microstructures that facilitated meteoric (especially water) and hydrothermal alteration. This allows us to conclude that bentonitization (alteration) is closely linked to the lithological characteristics of the rocks. In our sector, it develops essentially within the loose rhyolitic facies.

Scanning electron microscopy (SEM), Raman, infrared spectroscopy and X-ray diffraction (XRD) analyses carried out on the different facies in the study areas provide us with a set of results concerning bentonite that led us to the following conclusions:

The main components of bentonite are generally: montmorillonite, illite, calcite, hematite, sepiolite, fayalite, albite, biotite, orthose, cristobalite and calcite.

Non-clay minerals in the Tidiennit bentonite are represented in small quantities by feldspar and quartz. Whereas the clay minerals are represented by montmorillonite and illite, either in separate form or as an inter-layered illite-montmorillonite, of which montmorillonite occupies a significant volume of 80%.

In conclusion, it can be said that the mechanism of bentonitization is closely linked to both the intense brittle tectonics on any scale and the facies and dynamics of volcanism. These factors directly control the location, distribution and degree of bentonitization as a result of the combination of two factors generated by hydrothermal and/or meteoric circulation.

References

1. Noémie L. Contexte structural et métallogénique des skarns à magnétite des Beni Bou Ifrou (Rif oriental, Maroc) Apports à l'évolution géodynamique de la Méditerranée occidentale. Tectonics. Université d'Orléans. 2014 French. 1-476 (2015)
2. Hernandez, J., De Larouziere, F. D., Bolze, J., & Bordet, P., Le magmatisme néogène bético-rifain et le couloir de décrochement trans-Alboran. Bulletin de la Société Géologique de France, V. 3(2), 257–267 (1987)
3. Louaya A, Hamoumi N: Etude morphostructurale de la région de Nador Maroc nord-oriental. Africa Geoscience Review 172 :107–127 (2010)
4. Maychou S., Étude morphostructurale et cartographie SIG du Rharb Septentrional et du Prérif Maroc. Analyse sismotectonique et modélisation de la déformation de la région demoulay Boussselham. Thèse de doctorat de l'université Chouaib doukkali, El Jadida. (2009)
5. El Bakkali, S.: Volcanologie et Magmatologie du système du Gourougou (Rif Oriental, Maroc), France : Université de Clermont-Ferrand 2. Thèse nouveau doctorat.. Editeur [S.l.]. 285 (1995)
6. Viland J. C., Notes du Service géologique du Maroc, 37. 267(1977)
7. Aït Brahim L. and Chotin P.: Oriental Moroccan Neogene volcanism and strike-slip faulting. J.A.E.S, Vol. 11, No. ¾. 273-280(1990)
8. Hernandez J.: Le volcanisme miocène du Rif oriental (Maroc). Géologie, pétrologie et minéralogie d'une province shoshonitique. Ph. Doctoral Thesis, Univ. Pierre et Marie CURIE, ParisVI. 592 (1983)
9. Mourtajii.A.: Pre-feasibility study of the Tidiennit perlite deposit. Seminar on feasibility studies for mining projects the arab world . 8- 25 (1988)
10. Alaoui Mdaghri, D.Guerraoui, M. Bensaïd, Mand Damani,M.; Minister of energy and mines geology direction. Geological Service of Morocco edition. Memoir Note N°370 Maquette ((1992) and published ((1996)
11. Dehgani, Z.; Ghaedi, M.; Sabzehmeidani, M.M.; Adhami, E. Removal of paraquat from aqueous solutions by a bentonite odified zero-valent iron adsorbent. New J. Chem. 44, 13368–13376(2020)
12. Ait Hmeid, H.; Akodad, M.; Aalaoul, M.; Baghour, M.; Moumen, A.; Skalli, A.; Daoudi, L. Particle size distribution and statistic analysis of the grain size messinian bentonite from the kert bassin (northern Morocco). Mater. Today Proc.13, 505–514. (2019)
13. Inglethorpe SDJ, Morgan DJ, Highley DE, Bloodworth A. British Geological Survey: Industrial Minerals Laboratory Manual. Journal of Mathematics pp 124. (1993)
14. Christidis, G.E., Scott, P.W., Marcopoulos, T. Origin of the bentonite deposits of eastern milos, aegean, greece: geological, mineralogical and geochemical evidence. Clays and Clay Minerals. 43:63–77.(1995)
15. Rosenquist, I.Th.: Montmorillonitt fra Skyverdaleni Hemseedal. Norsk Geologisk Tidsskrift. 39, 350 (1959)
16. El Bakkali S, Gourgaud A, Bourdier JL, Bellon H, Gundogdu N. Post-collision neogene volcanism of the Eastern Rif Morocco: Magmatic evolution through time. Lithos 45:523-543(1998)
17. Hernandez J, Bellon H. K-Ar radiometric chronology of Miocene volcanics in eastern Morocco: tectonic and magmatologic. Revue de Geologie Dynamique et de Geographie Physique 262 :85-94(1985)
18. Ddani M, Meunier A, Zahraoui M, Beaufort D, EL Wartiti M, Fontaine C, Boukili B, El mahi B. Clay mineralogy and chemical composition of bentonites from the gourougou volcanic massif.(2005)
19. Lahrach M.N., & Malecha A.: Rapport inédit du BRPM. 461 (1985)
20. Mourtajii.A.: Pre-feasibility study of the Tidiennit perlite deposit. Seminar on feasibility studies for mining projects the arab world . 8- 25 (1988)
21. Rotella M, Simandl G. Marilla perlite - volcanic glass occurrence , british Columbia, Canada. Industrial Minerals with emphasis on Western North America, 263–272 (1996)
22. Mitropoulos, P., TARNEY, J., SAUNDERS, A.D. And MARSH, N. G. :Petrogenesis of cenozoic rock of Aegean Island Arc. Journal of Volcanism and Geothermal Research, 32.177-193 (1987)
23. Hawkesworth, C.J., Vollmer, R.: Crustal contamination versus enriched mantle: 143Nd/144Nd and 87Sr/86Sr evidence from the Italian volcanics. Contr. Mineral. and Petrol. 69, 151–165 (1979)
24. Sunders, P.; TARNEY, J. and D.WEAVER, S. Transverse Geochemical Variations Across The Antarctic Peninsula: Implications For The Genesis Of Calc-Alkaline Magmas. 11(1980)
25. Wood D A; Joron, Jean Louis; Treuil, M; Norry, Michael J; Tarney, J: Chemical composition and isotopic ratios of basic lavas from Iceland and the surrounding ocean floor. PANGAEA (1979)
26. Pearce, J.A., 1983. Role the subcontinental lithosphere in magma genesis of continental margin. In: Hawkesworth, C.J., Norry, N.J. _Eds., Continental Basalts and Mantle Xenoliths Shiva, Nantwich, pp. 230–249.
27. Blumenfeld, B.J.; A.L.S. Angelis, Besch, H-J.; Camiller, L.; Chapin, T.J.; R.L. Cool; Del Papa, C.; Di Lella, L.; Dimcovski, Z.; Hollebeek, R.J.; Lederman, L.M.; Levinthal, D.A.; Linnemann, J.T.; Newman, Phinney, C.B.; Pope, B.G.; Porde, S.H.; Rothenberg, A.F.; Rusack, R.W.; Segar, A.M.; Singh-Sidhu, J.; Smith, A.M. Tannenbaum, M.J. Vidal, R.A.; Wallace-Hadrill, J.S.; Yelton J.M.; And Young, K.K.: A measurement of the transverse momenta of partons, and of jet fragmentation as a function of \sqrt{s} in p-p collisions. Physics Letters B. Volume 97, Issue 1, 17 November 1980. 163-168 (1980)

28. Rachidi, M.; Étude géologique et minéralogique des secteurs Trébia, Prévencia, Taghzout (massif de Tidiennit) memoire Master .59 (2015)
29. Blumenfeld, B.J.; A.L.S. Angelis, Besch, H.-J.; Camiller, L.; Chapin, T.J.; R.L. Cool; Del Papa, C.; Di Lella, L.; Dimcovski, Z.; Hollebeek, R.J.; Lederman, L.M.; Levinthal, D.A.; Linnemann, J.T.; Newman, Phinney, C.B.; Pope, B.G.; Porde, S.H.; Rothenberg, A.F.; Rusack, R.W.; Segar, A.M.; Singh-Sidhu, J.; Smith, A.M. Tannenbaum, M.J. Vidal, R.A.; Wallace-Hadrill, J.S.; Yelton J.M.; And Young, K.K.: A measurement of the transverse momenta of partons, and of jet fragmentation as a function of \sqrt{s} in p-p collisions. *Physics Letters B*. Volume 97, Issue 1, 17 November 1980. 163-168 (1980)
30. Hajjaji M, Kacim S, Boulmane M 2002. Mineralogy and firing characteristics of a clay from the valley of Ourika Morocco. *Applied Clay Science* 213/4: 203–212. <https://doi.org/10.1016/S0169-131701.00101-6>.
31. Mehdi F., Modification de la bentonite par un sel de diposphonim applications à l'adsorption des colorants textiles rouge, bleu et jaune Bemacide. . Mémoire du master de l'université Abou bekr belkaid, Tlemcen. (2014)
32. Nayak, P.S.; Singh, B.K. Instrumental characterization of clay by XRF, XRD and FTIR. *Bull. Mater. Sci.* 30, 235–238.(2007)
33. Cariati F, Erre L, Micera G, Piu P, Gessa C. Water molecules and hydroxyl groups in montmorillonites as studied by near infrared spectroscopy. *Clays and Clay Minerals*. 29:157-159 (1981)
34. Gupta A, Amitabh V, Kumari B, Mishra B. FTIR and XRPD Studies for the Mineralogical Composition of Jharkhand. *Research Journal of Pharmaceutical*. (2013)
35. Zahaf, F. Etude Structurale des Argiles Modifiées Appliquées à l'Adsorption des Polluants. Ph.D. Thesis, University Mustapha Stambouli of Mascara, Mascara, Algeria. (2017)
36. Boufatit, M.; Ait-amar, H.; Mcwhinnie, W.R. Development of an Algerian material montmorillonite clay. Adsorption of phenol, 2-dichlorophenol and 2,4,6-trichlorophenol from aqueous solutions onto montmorillonite exchanged with transition metal complexes. *Desalination*, 206, 394–406. (2007)
37. Kumpulainen, S.; Kiviranta, L. Mineralogical and chemical characterization of various bentonite and smectite-rich clay materials-Part A: Comparison and development of mineralogical characterization methods—Part B: Mineralogical and chemical characterization of clay materials. *Posiva. Oy.*, 52, 74. (2010)
38. Khenifi, A. ; Elaboration de Matériaux à Base d'Argiles, Caractérisation, et Application à l'élimination des Polluants Organiques. Ph.D. Thesis, University of Science and Technology of Oran Mohamed Boudiaf, Oran, Algeria, (2010)
39. Akcay, G.; Yurdakoc, K. ; Nonyl-and dodecylamines intercalated bentonite and illite from Turkey. *Turk. J. Chem.*, 23, 105–114. (1999)
40. Bouras, O. ; Propriétés Adsorbantes d'Argiles Pontées Organophiles: Synthèse et Caractérisation. Ph.D. Thesis, University of Limoges, Limoges, France, (2003)
41. Balci S, Gokcay E. Pore structure and surface acidity evaluation of Fe-PILCs. *Turkish Journal of Chemistry* 33:843–856.(2009)
42. Ravindra Reddy, T.S.; Endo, K.T.; Lakshmi Reddy, S. Spectroscopic characterization of bentonite. *J. Lasers Opt. Photonics*, 4, 1–4. (2017)
43. Brahimi, S.; Boudjema, S.; Rekkab, I.; Choukchou-Braham, A.; Bachir, R. Synthesis and catalytic activity of vanadia-doped iron-pillared clays for cyclohexene epoxidation. *Res. J. Pharm. Biol. Chem. Sci.* 6, 63–76. (2015)
44. Hayati-Ashtiani, M.; Characterization of nanoporous bentonite (montmorillonite) particles using FTIR and BET-BJH analyses. *Part. Syst. Charact.* 28, 71–76 (2011)